PROCEEDINGS OF SPIE

SPIEDigitalLibrary.org/conference-proceedings-of-spie

Miniaturized silicon photonics multi-sensor operating at high temperatures for use in composite materials industrial applications

Zervos, Charalampos, Poulopoulos, Giannis, Missinne, Jeroen, Szaj, Michal, Avramopoulos, Hercules

Charalampos Zervos, Giannis Poulopoulos, Jeroen Missinne, Michal Szaj, Hercules Avramopoulos, "Miniaturized silicon photonics multi-sensor operating at high temperatures for use in composite materials industrial applications," Proc. SPIE 12008, Photonic Instrumentation Engineering IX, 120080P (5 March 2022); doi: 10.1117/12.2606053

SPIE.

Event: SPIE OPTO, 2022, San Francisco, California, United States

Miniaturized silicon photonics multi-sensor operating at high temperatures for use in composite materials industrial applications

Charalampos Zervos[a], Giannis Poulopoulos[a], Jeroen Missinne[b], Michal Szaj[c], Hercules Avramopoulos[a]
[a]Photonics Communications Research Laboratory National Technical University of Athens, Greece;
[b]Center for Microsystem Technology (CMST) Ghent University and imec Ghent, Belgium;
[c]Argotech a.s. Trutnov, Czech Republic;

ABSTRACT

Composite materials offer significant performance advantages due to their lightweight, high-strength, and high stiffness. This led to their adoption in several industrial sectors with particular emphasis on the aerospace industry which has undergone a transformation towards a composite-dominated new standard. In order to respond to the increased demand, it is mandatory to focus on an efficient and well-controlled curing cycle of the resin, which will lead to a significant reduction of cost and an increase in production speed. Currently, manufacturers use filling and curing cycles with high safety margins which can be optimized by applying process monitoring techniques, which up to now use thermocouples and dielectric sensors. However, these electric solutions suffer in terms of operating capabilities and the facilitation of integrating them in composite materials (due to their size and electrically conductive aspect when using carbon fibers).
We present the design and evaluation of a miniaturized novel photonic integrated sensor, fabricated in 220 nm top SOI platform, capable of measuring key monitoring values that facilitate optimization of the curing process. The operation principle is the spectral shift of a silicon Bragg grating component's resonant wavelength. Bragg grating design and post-processing of the integrated chip allows for measuring different key values such as temperature, refractive index and pressure all in ~1.5 mm diameter. The fabricated temperature sensors achieve a significant 0.084 nm/°C thermo-optic efficiency with high accuracy (0.5 °C) and repeatability across a very wide dynamic range (temperature 27 to 180 °C).

Keywords: Photonic sensor, composite material fabrication, Bragg grating, wide dynamic temperature range, miniaturized multi sensor, composite molds, silicon photonics, temperature sensor

1. INTRODUCTION

The performance advantages offered by composites over traditional materials, specifically lightweight, high strength, and high stiffness, has led to their growing adoption in several industrial sectors. They are ideal materials for those applications requiring highly advanced technologies, such as aircraft and automotive parts [1], but also for construction and infrastructure elements. The aerospace industry has undergone a transformation from a metal-driven world to a composite-dominated new standard [2], while the automotive industry has also been increasingly using composites for their cost and weight reduction and recyclability advantages [3]. The major drivers for growth in the composite market are represented by the increasing demand for lightweight materials in the aerospace and automotive industries [4]. To cater to the increase in this demand two considerations must be focused on in the composite industry, a) The efficient and controlled curing cycles to reduce costs and speed up production and b) the adoption of composite tools (molds) for their lower (10x less than metal tools), ease of movement, ease of construction, and lower price, compared to standard metal tools [5]. The sensor concept which is presented facilitates both of the abovementioned considerations. In regards to point a) above, currently, most manufacturers use standard filling and curing cycles with high safety factors to determine the cure duration. Long curing times lower the productivity and can imply a risk of products not fully being cured. Optimization of the filling and curing cycles and, thus, increase productivity, by applying process monitoring techniques are already available in the market, like thermocouples and dielectric sensors. However, these electric solutions suffer in terms of operating capabilities as well as being unsuitable to be integrated within electrically conductive tool, using carbon fibers for reinforcement for example. In relation to b) and the shifting of the industry to using composite tools, the deployment of sensors in these tools can be challenging and can alter the structural integrity of the tool resulting in composite parts that are of lower quality and this is mainly due to the size or material of the sensors, for which commonly drilling is required in order to be mounted in the tool. The presented concept capitalized on the

Photonic Instrumentation Engineering IX, edited by Lynda E. Busse, Yakov Soskind, Proc. of SPIE Vol. 12008, 120080P · © 2022
SPIE · 0277-786X · doi: 10.1117/12.2606053

miniaturization aspect of the photonic sensor, which is ~1.5 mm in diameter packaged, in order to ensure a seamless integration of the sensor in the composite tool during its fabrication stage. In this paper, in Section 2 the overall concept of the photonic multi sensor will be presented as well as how it designed to be integrated into composite tools. In Section 3 the design considerations and methodology of a Bragg based Temperature sensors are presented along with simulation results. Finally in Section 4 the testbed for testing such a temperature sensor is presented using an interrogator commonly used in the composite industry for Fiber Bragg sensors as well as initial measurements showing a significant thermo-optic efficiency of 0.084 nm/°C thermo-optic with high accuracy (0.5 °C) and repeatability across a dynamic range of 27 to 180 °C, corresponding to the temperature range required to use composite tools.

2. CONCEPT OF SENSOR

As it has been mentioned in Section 1, composite parts manufacturing cycles depend significantly on tool heating and cooling rates and a controlled process will result in increased production and quality of composite materials. The presented multi sensors will achieve this by appropriate cure and flow monitoring of material parameters through the development of self-monitoring composite tool for resin transfer molding (RTM) infusion processes. Specifically for the sensor, a multi-sensor Photonic Integrated Circuit (PIC) is shown, embedded in a composite tool using Through Thickness Reinforcement (TTR) techniques, employing Bragg based sensor design (presented in Section 3).

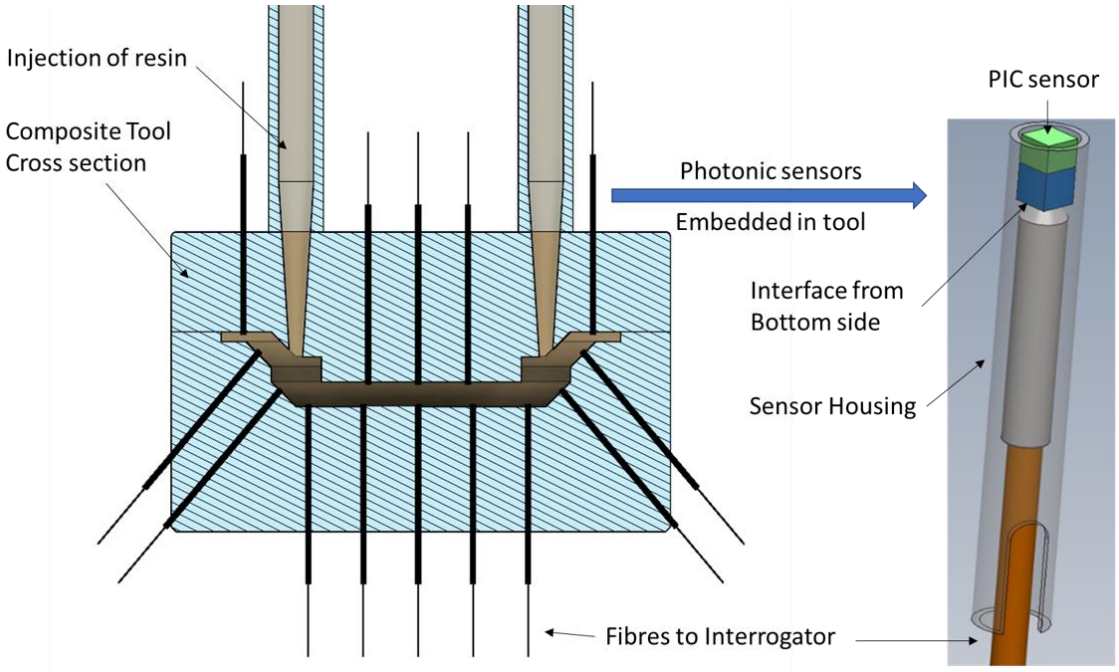

Figure 1. Cross sectional view of the composite mold (tool) where the injection funnels for the resin and the embedded photonic sensor modules are shown both in the "punch" (top side of the mold) and the "matrix" (bottom side of the mold). A zoomed in schematic of a single sensor module is shown, with the PIC sensor sitting on the top, the interface to a single SMF fiber on the bottom of the PIC and the housing that encloses the sensor assembly is denoted. The sensor is embedded in the composite mold using Through Thickness Reinforcement (TTR) techniques in its housing. The interrogator is one that is produced for use in the composite industry and for monitoring Fiber Bragg strain sensors.

Figure 1 shows a cross section of a composite tool (mold) with embedded photonic sensors. The PIC is situated on the top of the sensor module and it comes into contact with the manufactured composite part. This allows the photonic sensor to measure Refractive Index (RI) through changes in the evanescent field of a Bragg sensing element and measure pressure (p) by incorporating a cavity underneath a different Bragg sensing element. This setup is using only one fiber to couple the light in and out and it requires access to the PIC from the bottom side.

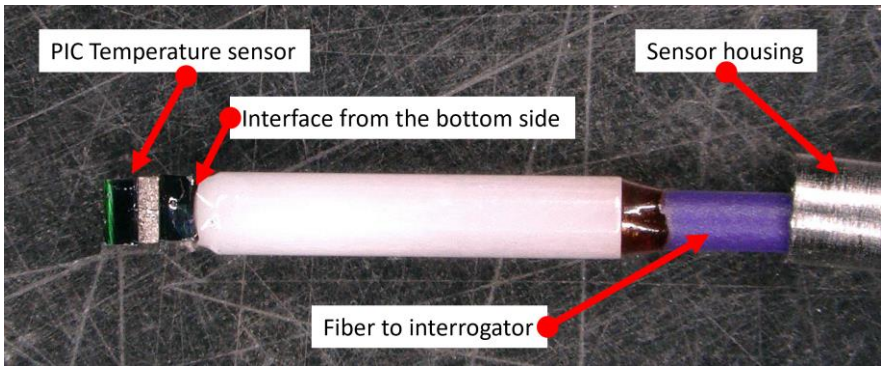

Figure 2. A picture of the Temperature Photonic sensor assembled. The sensor assembly is pulled out of its housing so that the interface can be shown.

Figure 2 shows a picture of a Temperature (T) sensor that has been assembled following the above-mentioned scheme. Temperature sensors from the same fabrication run have been measured and results are presented in Section 4. By using slightly different λ_B (Bragg wavelength that is reflected) for multiple Bragg grating-based sensing elements in order to reflect different wavelengths for different quantities i.e. T, RI and p, the multi-sensor is implemented in a single PIC. A conceptual layout of the three Bragg based sensors on a single PIC is shown in Figure 3 from the Top, while a cross-sectional view of the PIC shows the concept of realizing different sensors, i.e. a T sensor, an RI sensor with exposure to the resin and a p sensor with a cavity in the Si substrate.

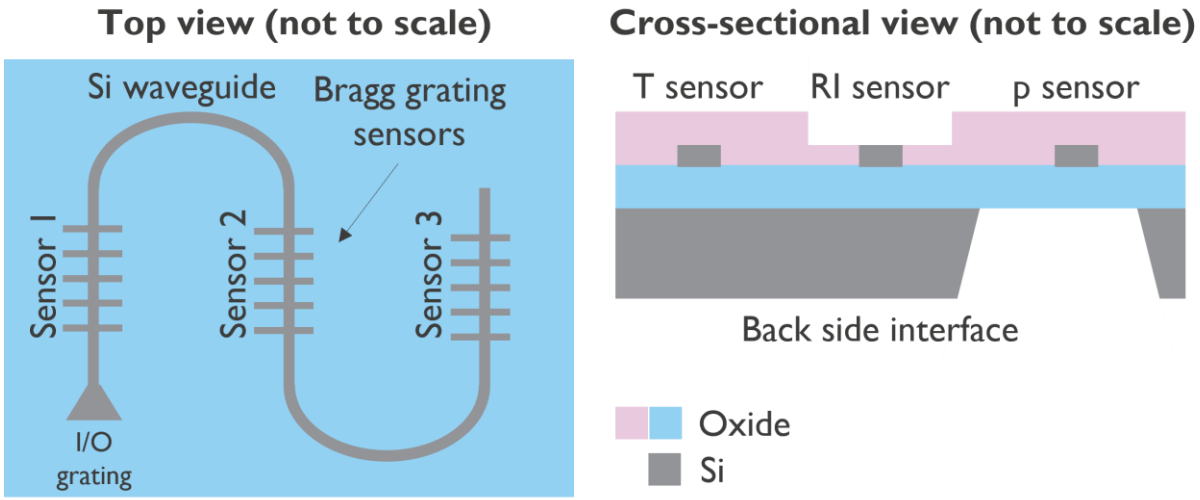

Figure 3. The concept of a single PIC multi sensor is shown not to scale to illustrate better the underlying concepts. In the Top View on the left, the three sensors are placed in series, with an Input/Output grating coupler. Each Bragg sensor is designed so that the reflected wavelength is different to allow all three to be multiplexed in a single PIC. In the Cross-sectional view on the right, each sensor is processed in a different way to allow sensing different qualities. The RI sensor is exposed to the resin on the top by etching the top oxide layer, while the bottom Si substrate has a cavity on the p sensor to allow mechanical movement underneath the sensor.

The photonic sensor is designed to have a dynamic range, resolution and accuracy based on requirements of the Resin Transfer Molding (RTM) process for manufacturing composite parts. For the temperature sensor these values are displayed in Figure 4.

Parameters	***Dynamic Range***	***Resolution***	***Accuracy***
Temperature	Ambient – 180 ºC	0.1 °C	1 °C

Figure 4. Table showing the Dynamic Range, Resolution and Accuracy targets for Temperature (T). These have been set based on the requirements of the Resin Transfer Molding (RTM) fabrication process for composite materials

The rate of change that is required is based on the application of the composite part that will be manufactured. For our purposes in aerospace, where quality control of the process is the priority, the fabrication of composite parts has typical single cycle duration in the order of a few hours. This is well within the speed that the photonic sensor acquires data considering the sampling rate lies at the kHz level. This fact makes the photonic sensors suitable for automotive applications as well which that has duration cycles in the order of minutes.

In this paper and in the following sections the focus is on the design and testing of the temperature sensors, which was the first step into realizing this multi sensor concept.

3. TEMPERATURE SENSOR DESIGN

In this section, the design methodology of Bragg grating structures, as well as their performance on temperature sensing operation, are presented. Bragg grating is a photonic element characterized by periodic modulation of refractive index (RI), across propagation direction, while at each refraction change, a small amount of light of certain wavelength is reflected. All the reflected light signals combine coherently to one large reflection at a particular wavelength at element's input. This is referred to as the Bragg condition, and the wavelength at which this reflection occurs is called the Bragg resonance wavelength. Bragg grating structures are designed for 220 nm Silicon On Insulator (SOI) technology. The design parameters that can be modified are the pitch (period) of the grating (Λ), corrugation width (*dw*), Filling Factor *(FF*), and effective index of propagation mode (n_{eff}). In our study only Bragg grating structures with *FF* value equal to 50% will be investigated. The resonance wavelength value (reflected wavelength) can be calculated via Bragg equation:

$$\lambda_{res} = 2 \cdot n_{eff} \cdot \Lambda$$

A schematic of a 50% FF Bragg grating structure, as well as its design parameters, is shown in Figure 5.

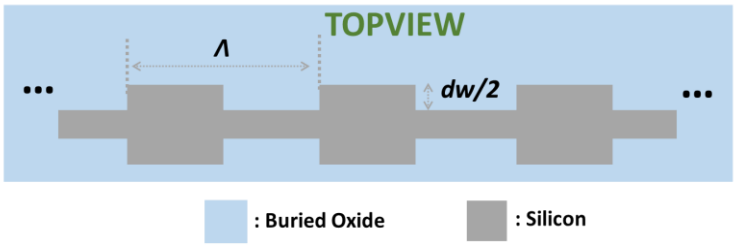

Figure 5. Top view of Bragg grating photonic element

The electromagnetic simulation software for mode calculations and propagation simulations used, is the commercially available Ansys Lumerical MODE Solutions [6]. The 220 nm top SOI platform supports both TE and TM polarization mode, whereas the nominal waveguide width is 450 nm and 500 nm for TE and TM polarization, respectively. The refractive index values for the layerstack materials are 3.47 for silicon waveguide, 1.45 for Buried Oxide layer, and 1.41 for cladding layer.

By appropriately choosing values for the aforementioned design parameters, spectral response of the Bragg grating element can be calculated. EigenMode Expansion (EME) propagation solver was employed to calculate the reflection spectral response of a TE Bragg grating structure characterized by 320 nm pitch, 10 nm corrugation width, and 200 number of periods. Spectral response of this Bragg grating is plotted versus wavelength as the black line of the leftmost graph of Figure 6. As can be shown in Figure 6, by varying design parameters of the Bragg grating structure, specific changes of the spectral response occur, and more specifically:

- Varying grating pitch (Λ) → resonance wavelength is shifted
- Varying corrugation width (dw) → spectral bandwidth changes
- Varying Number of periods (N) → insertion loss value changes

To this end, a certain set of design parameters value is chosen, to comply with the specific requirements on wavelength shift, loss, and bandwidth of each use case requirements.

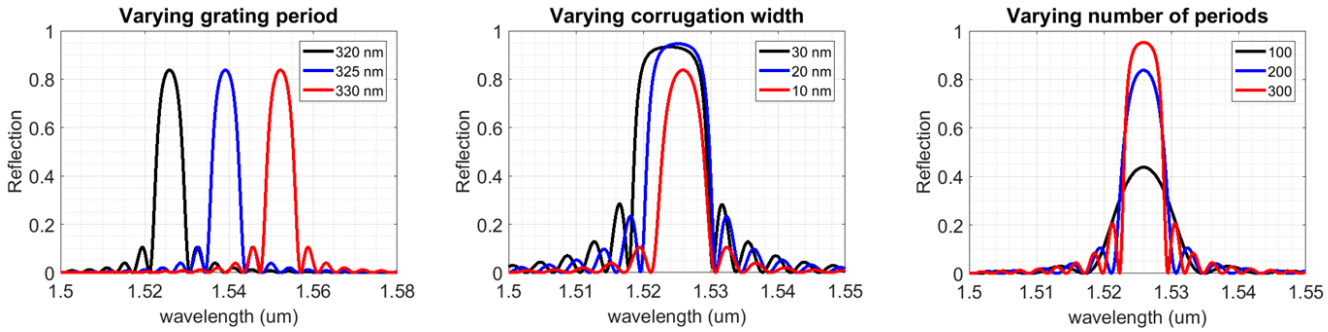

Figure 6 Effect on spectral response, varying Bragg grating design parameters

More specifically, in Figure 7 a set of reflection spectra can be shown for TE polarization operation Bragg grating structures, as calculated employing EME propagation solver for 220 nm top SOI waveguides and 450 nm nominal width. The effective index value as calculated for 450 nm width waveguides was calculated to be 2.3517. As can be seen in Figure 7(a), (c), and (d) the resonance wavelength is calculated to be 1532 nm, a result of the 324 nm period of Bragg gratings. By varying the corrugation width parameter of each Bragg grating, the 3-dB bandwidth is broadening with increasing the dw value (corrugation width). In Figure 7(b) the reflection spectrum of a Bragg grating with period value of 330 nm is shown, red shifted compared to the 324 nm period Bragg grating structures.

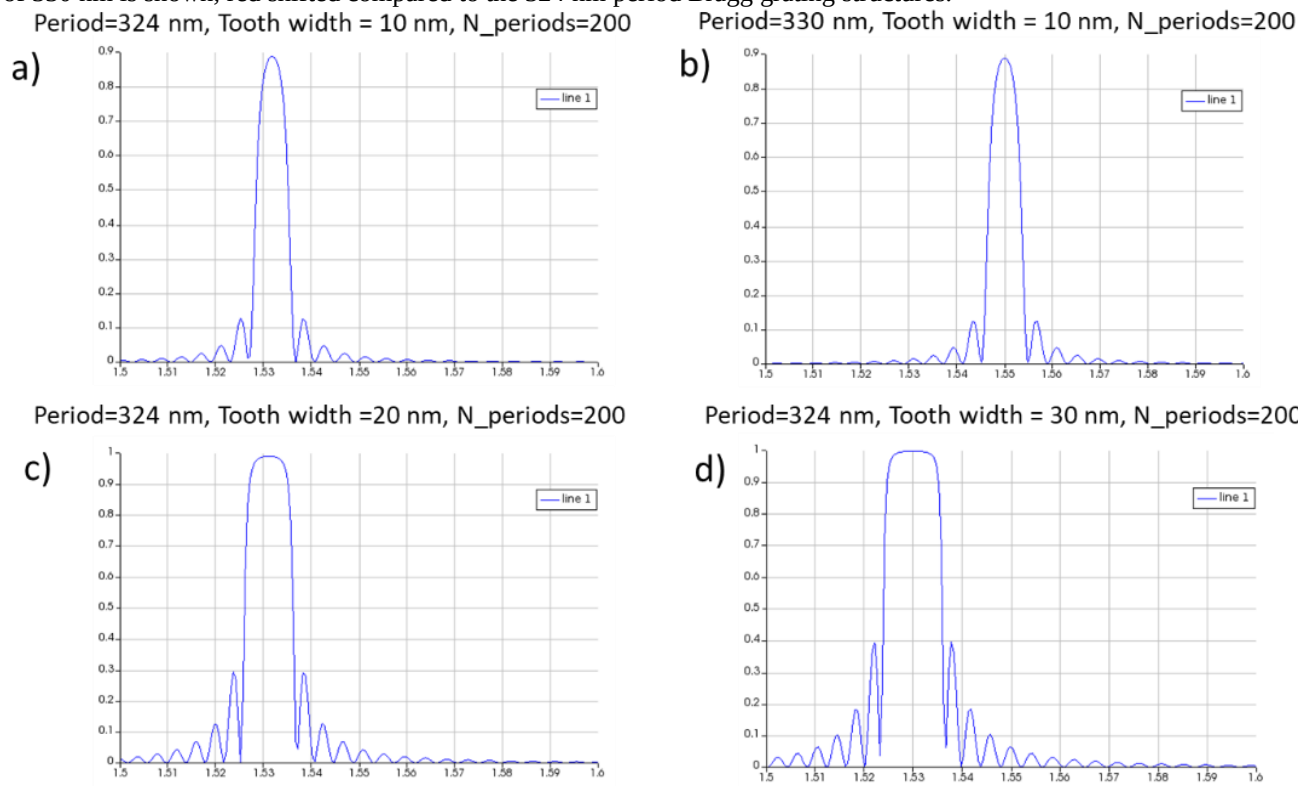

Figure 7. Calculated reflection spectrum for a series of TE polarization mode operation Bragg grating structures

After completing the Bragg grating element design, the thermo-optic response of these structures will be simulated. Temperature sensor is primarily based on thermo-optic effect, thus meaning exploiting the refractive index of silicon material by changing temperature. Thermo-optic coefficient of silicon is $\frac{dn}{dT} = 18 \times 10^{-5}\ \mathrm{K}^{-1}$ for wavelength values around 1.55 μm. Thermal sensitivity can be analytically calculated via the following equation for Bragg gratings:

$$\frac{d\lambda}{dT} = \frac{\lambda}{n_g}\frac{dn_{eff}}{dn}\frac{dn}{dT}$$

In this paragraph, instead of simulating the $\frac{dn_{eff}}{dn}$ fraction, to calculate thermal sensitivity, we carry out a set of thermal simulations to specify thermal sensitivity directly. Thermo-optical simulations were carried out in Mode Solutions Lumerical software for temperature range between 27 °C to 187 °C. The cross section of the silicon thermo-optic sensor is shown in Figure 8(a). Simulation results for a nominal TE polarization Bragg grating are shown in Figure 8(b), revealing the red-shift of resonance wavelength by increasing temperature.

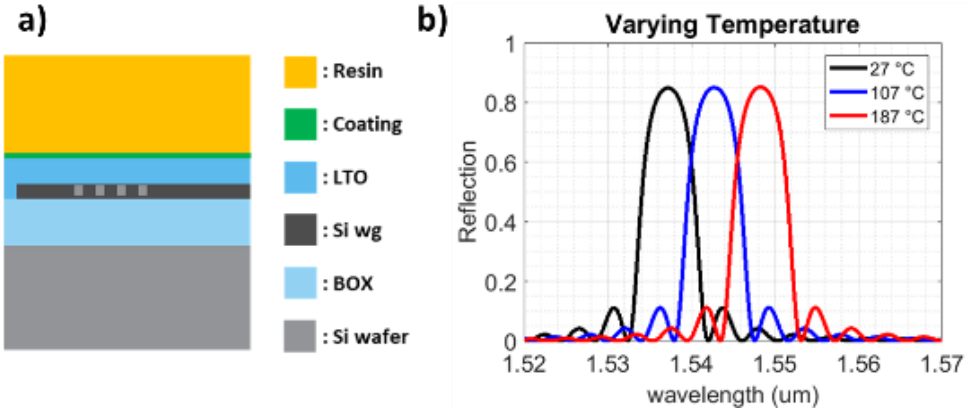

Figure 8.(a) Thermo-optic sensor cross section, and (b) Spectral response varying Temperature

A full set of thermo-optic simulations was then carried out for both TE and TM polarization mode. Wavelength shift is linear as shown in Figure 9, whereas the total wavelength shift (Temperature: 27 °C to 187 °C) is depicted for TE (blue line) and TM (red line) polarization operation. Thermo-optic wavelength tuning efficiency is simulated to be 0.070 nm/°C and 0.044 nm/°C for TE and TM polarization mode, respectively with accuracy of 0.5 °C.

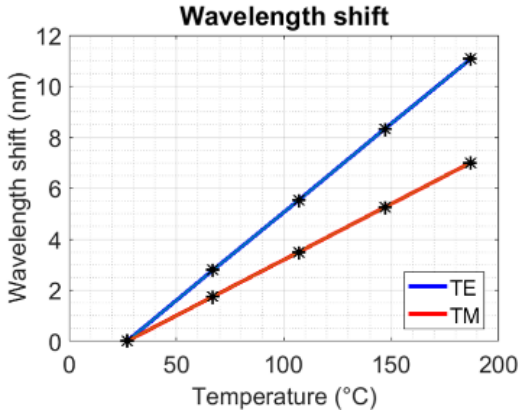

Figure 9. Wavelength shift varying temperature for TE and TM polarization operation

4. TESTBED AND RESULTS

In this paragraph the testbed to evaluate temperature sensing elements and the experimental results are discussed. As may be seen in Figure 10, a narrowband tunable laser is employed as light source provided by the FAZT I4G commercial interrogator. The interrogator covers 39.2 nm of C-band with a frequency of 2 kHz (1529 nm – 1568.2 nm). It operates on TE or TM polarization mode and for each wavelength it transmits, it measures the reflection optical power. The interrogator displays the whole spectrum, and it allows us to measure the exact resonance wavelength as well as the spectral characteristics of the Bragg grating reflection spectrum. The interrogator cannot be used to measure the exact power level of the reflection spectrum but only provides relative measurements. However, this is not critical for the evaluation measurements of the sensors which relies on the shift of the reflection resonance wavelength of the Bragg grating as the chip temperature varies.

As can be seen in Figure 10, an in-line fiber polarization controller (PC1) together with an in-line fiber polarizer, are used after the interrogator to align the interrogator output state of polarization with the 45° angle polarizer optical axis. By employing this configuration it is ensured that only a single state of polarization is transmitted after polarizer. A

second in-line fiber polarization controller (PC2) is then employed, to select the state of polarization at the fiber tip, just before entering the chip under test. The reflection then follows the opposite direction, starting from PC2, passing through polarizer and PC1, and reaching the interrogator to be monitored. Also, a through port power meter is employed, to facilitate the alignment of the fibers on top of chip under test. All fibers used across the testbed setup are SMF.

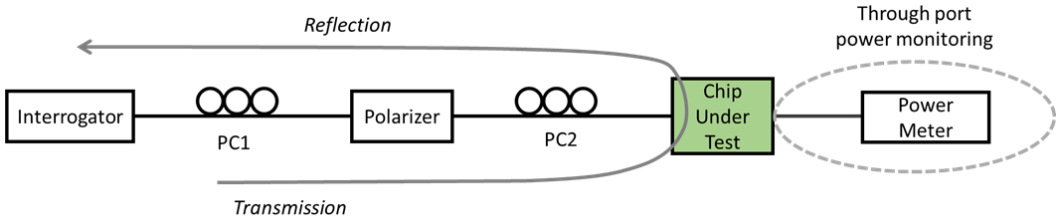

Figure 10. Testbed setup to measure reflection spectrum employing a FAZT I4G commercial interrogator

The testbed on which the chip is located, consists of 6-axis electrically controlled piezoelectric positioners, for the input and output fibers. The chip is located on a copper vacuum chuck to hold it firmly in place, which is embedded in the plated copper heater block. Fiber-to-chip alignment is enabled via optical inspection, using a camera on top of the chip, as well as via power monitor at the through port as already described. The heater block (plated copper block) hosts the vacuum chuck, an ohmic resistance heater as well as a temperature monitoring component. More specifically, in this bench setup, a ceramic heater with maximum power load of 30 W is embedded on the heater block, enabling temperature increase of the entire block up to 300 °C, while provides long-lasting and consistent performance. Cooling process is controlled via a fan placed next to the heater block. Temperature is then monitored via two processes, namely: a) employing a thermistor (Semitec 104GT2) which is capable of sensing up to 300 °C hosted on the heater block, and b) using a commercial FLIR thermometer (FLIR TG56) able to provide calibrated temperature measurements with high accuracy. The control of the heater and fan, as well as the monitoring of the thermistor is achieved via employing open-source code.

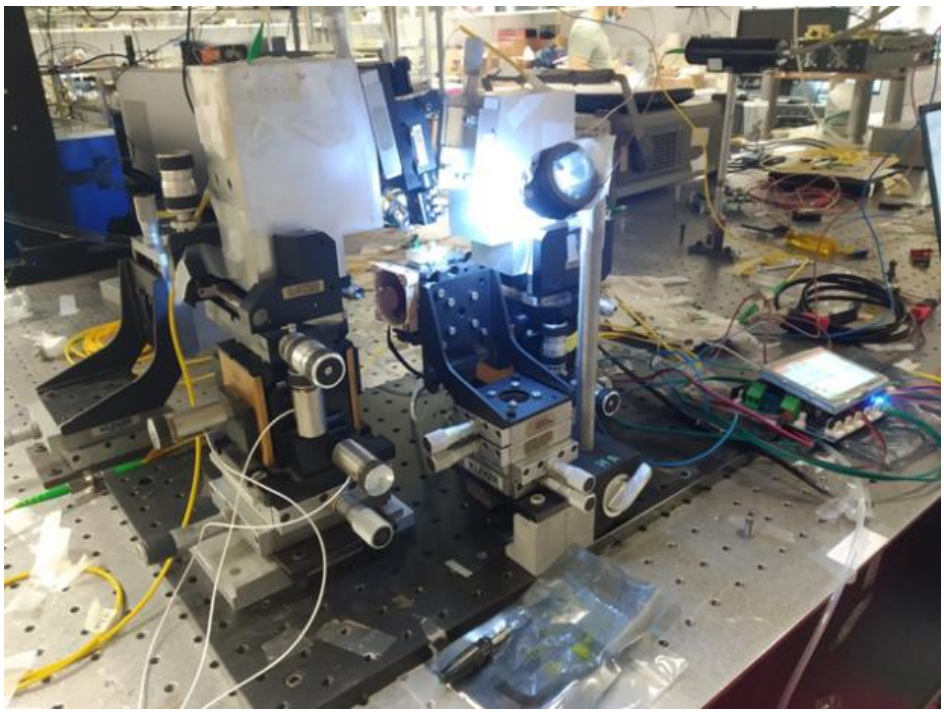

Figure 11. Bench setup for chip temperature evaluation measurements

Data on the reflection spectrum are acquired by the interrogator (at 4kHz), after both input and through port fibers are optimally aligned to silicon chip, and both polarization controllers aligned to minimize insertion losses and maximize fiber to chip coupling efficiency for TE polarization mode operation. The mean-values of a series of 10 reflection spectra is calculated from the acquired data. The mean-value helps to smooth out any data due to instantaneous vibrations of the chip and bench that the chip is placed, allowing a determination of the wavelength shift with easy, while still providing a

rate of measurement at 400 Hz. Before thermal load is applied to the heater, and thus chip temperature is increased, the chip temperature was measured to be 25.2 °C. Then, the chip temperature is increased from 25.2 °C to 40 °C, up to a maximum of 180 °C. The results are plotted in Figure 12, where the reflection spectra for 20 nm corrugation width gratings, with 200 periods of 324 nm in length varying chip temperature is shown. By increasing the chip temperature, the reflection spectrum is red-shifted. As can be seen, even for chip temperature of 180 °C, the reflection peak is in the range of interrogator reading spectrum, and thus the monitoring for all temperatures up to 180 °C is feasible for the 324 nm pitch grating. Difference of peak power levels after varying temperatures, even that as already mentioned the power levels can only be characterized as "relative", could be explained due to thermal expansion of silicon structures when they are heated, thus contributing to fiber-to-chip misalignment, as well as narrowband input grating coupler structures operation.

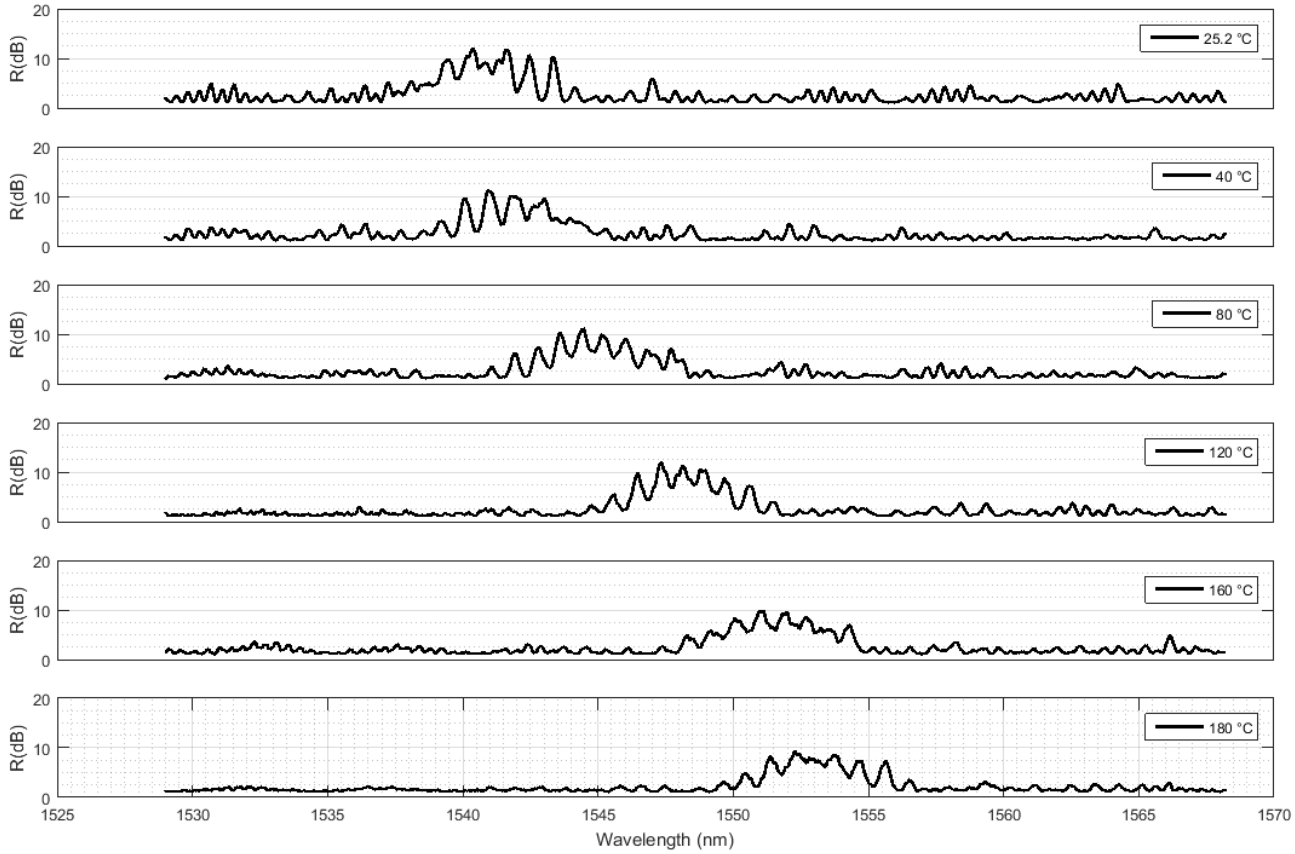

Figure 12. Reflection spectrum measurements varying chip temperature

The reflection spectrum is characterized by ripples which are due to reflections taking place at the fiber tip-to-grating coupler optical interface, and their effect can be minimized by employing phase matching liquid at this interface. It is expected that in the sensor concept presented in Section 2, where the optical interface assembly will be done using active alignment and employing Polarization Maintaining fibers, these ripples will be considerable reduced.

As may be seen in the linear regression line shown in Figure 13, a mean value of thermo-optic tuning efficiency of 0.084 nm/°C is measured, characterized by high linearity (R^2 = 0.99728), while this value has the potential to further e enhanced by optimizing the fiber-to-grating coupler interface as explained above.

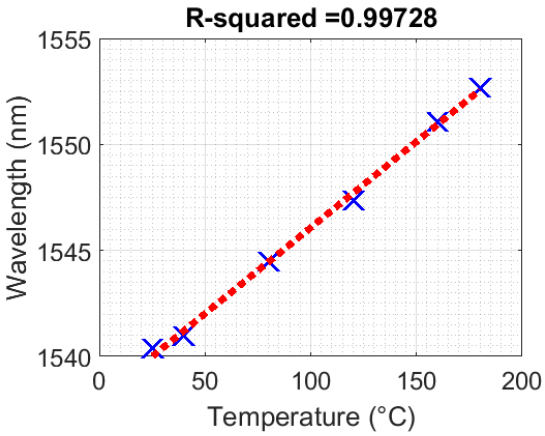

Figure 13. Resonance wavelength varying temperature, and its linear regression

Regarding the resolution value specification of the designed Bragg grating structures designed and fabricated, as it is also affected from the temperature control and measurement system employed. The TE polarization mode operation phase-shifted Bragg grating, with 20 nm corrugation width, 324 nm pitch and 200 periods length was selected. We set the chip temperature measurements to take place around 120 °C, with a 0.5 °C step. Reflection spectra of this Bragg structure varying temperature from 119 °C to 121 °C, with a 0.5°C step, are plotted and shown in Figure 14. Note that the horizontal axis is limited in the wavelength range between 1547.2 nm and 1548 nm.

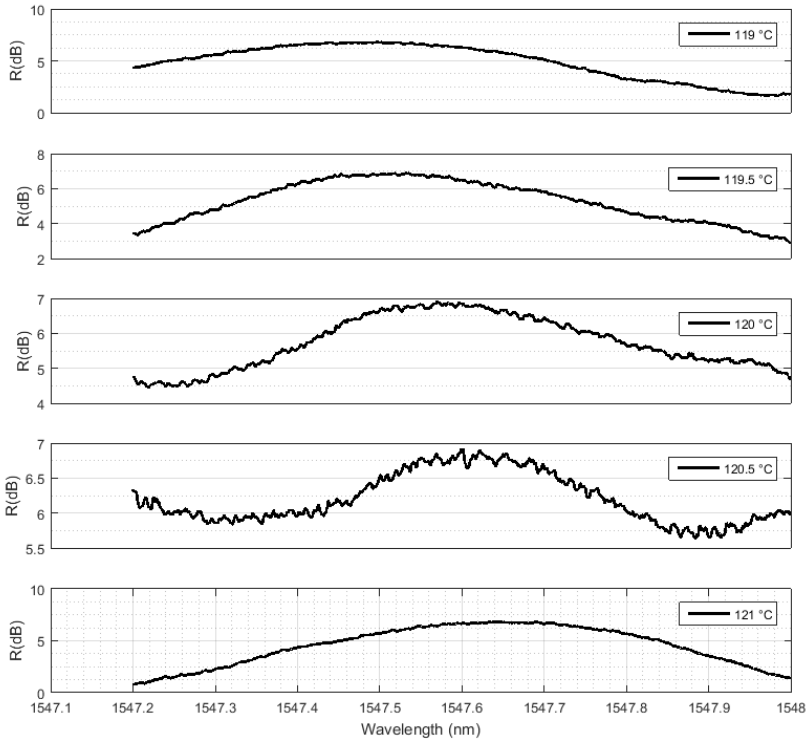

Figure 14. Reflection spectra for resolution measurements around 120 °C, with 0.5 °C step.

The reason for this limited wavelength range is only illustrative, to have a magnified view on the relevant reflection spectra peaks. As may be seen in Figure 15, an R^2 value of 0.98717 is achieved for these resolution measurements around 120 °C, with 0.5 °C step.

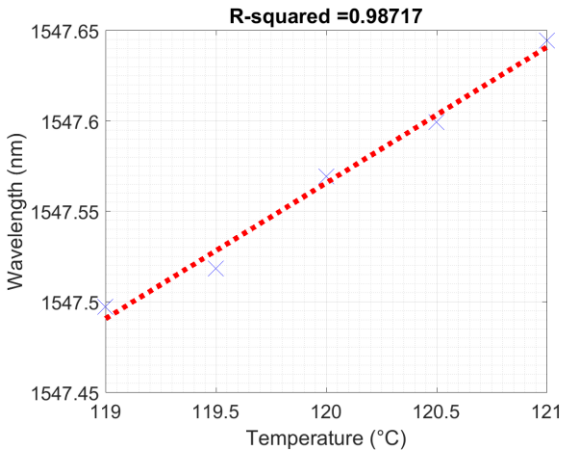

Figure 15. Resonance wavelength varying temperature for resolution specification, and linear regression values

5. CONCLUSIONS

We present the design and evaluation of a miniaturized novel photonic integrated sensor, capable of measuring key monitoring values that facilitate optimization of the curing process. The fabricated temperature sensors achieve 0.084 nm/°C thermo-optic efficiency with high accuracy (0.5 °C) across a very wide dynamic range (temperature 27 to 180 °C). Future work on these Bragg grating sensors will be focused on design and fabrication of phase-shifted Bragg grating elements targeting even greater accuracy and sensitivity values. Moreover, by increasing the temperature dynamic range above 180 °C, the sensor will prove its ability to operate to a wider variety of composite material applications.

REFERENCES

[1] https://www.ncbi.nlm.nih.gov/pmc/articles/PMC5796376/
[2] http://compositesmanufacturingmagazine.com/2018/01/2018-composites-manufacturing-state-of-the-industry-report/
[3] https://compositesuk.co.uk/composite-materials/applications/automotive
[4] https://www.prnewswire.com/news-releases/global-composites-industry-overview-2018-2023---increasing-demand-for-lightweight-materials-in-the-aerospace--defense-and-automotive-industry-300673139.html
[5] https://info.dte.co.uk/why-composite-materials-are-the-best-thing-for-the-automotive-sector
[6] https://www.lumerical.com/